PHYSICAL REVIEW D **74,** 124020 (2006)

Gauge theory in de Sitter space-time from a holographic model

Kazuo Ghoroku,[1] Masafumi Ishihara,[2] and Akihiro Nakamura[3]

[1]*Fukuoka Institute of Technology, Wajiro, Higashi-ku Fukuoka 811-0295, Japan*
[2]*Department of Physics, Kyushu University, Hakozaki, Higashi-ku Fukuoka 812-8581, Japan*
[3]*Department of Physics, Kagoshima University, Korimoto 1-21-35, Kagoshima 890-0065, Japan*

(Received 22 September 2006; published 20 December 2006)

Yang-Mills (YM) theory with flavor quarks in the dS_4 is studied through the dual supergravity in the $AdS_5 \times S^5$ background with nontrivial dilaton and axion. The flavor quarks are introduced by embedding a probe D7 brane. We find that the dynamical properties of YM theory in the dS_4 are similar to the case of the finite temperature theory given by the 5d AdS-Schwarzschild background. In the case of dS_4, however, contrary to the finite temperature case, the gauge-field condensate plays an important role on the dynamical properties of quarks. We also give the quark-antiquark potential and meson spectra to find possible quark-bound states. We arrive at the conclusion that, while the quarks are not confined in the dS_4, we could find stable meson states at very small cosmological constant as expected in the present universe. However, there would be no hadrons at early universe as in the inflation era.

DOI: 10.1103/PhysRevD.74.124020 PACS numbers: 04.50.+h, 04.62.+v, 04.65.+e, 11.25.Mj

I. INTRODUCTION

Recently, there have been many approaches to QCD from the gauge/gravity correspondence based on the superstring theory [1]. Especially, the idea, proposed by Karch and Katz [2], to add light flavor quarks by embedding D7 brane(s) as probe has stimulated many authors who have developed and extended this idea to various 10d gravity solutions corresponding to the various gauge theories. Many interesting results have been obtained for the properties of quarks and their bound states, mesons, in the context of the holography [3–10].

This approach has been developed in many directions, but the analyses are restricted to the gauge theory in 4d Minkowski space-time and to the finite temperature theory. On the other hand, some holographic approaches to the gauge theory in the 4d de Sitter space (dS_4) are seen [11–14], but it is not enough and we will need more study. This situation of the positive cosmological constant can be set for the early inflation universe or for the present small acceleration which has been observed recently in our universe. From this cosmological viewpoint, it would be important to make clear the nonperturbative properties of the gauge theories at finite cosmological constant. It would be a difficult problem to see the nonperturbative behaviors of field theories in a curved space from the standard field theory, so this problem is a challenging one.

Here we study this problem from the holographic approach which has been useful in the finite temperature case [9]. The bulk solution corresponding to the gauge theory in dS_4 is obtained from type IIB string theory with dilaton and axion under the five-form flux. And the D7 brane is embedded in this background as a probe to introduce the flavor quarks. In the bulk background, there appears a horizon as in the finite temperature case. And we find an attractive force between D3 and D7 branes, then the chiral symmetry is preserved as in the high temperature phase. But a phase transition observed in the high temperature case is seen only for the case of large gauge-field condensate. For small gauge condensate, it is deformed to a different situation which has not seen in the finite temperature case.

In order to study the quark confinement, we obtained the potential between quark and antiquark through the estimation of the Wilson-Polyakov loop. We find a maximum distance between quark and antiquark to maintain the U-shaped string state. Above this length, the quark and antiquark are separated as independent particles. And the energy of each single quark (or antiquark) state is finite. This point is assured through the estimation of the effective quark mass. Then, in this sense, we can say that the theory is in the deconfinement phase. We compare these results with the one given at the finite temperature.

Furthermore, we estimate the meson masses through the fluctuation of the D7 brane, and we find interesting spectra for light mesons. However, all the states would disappear at large cosmological constant since they becomes unstable and decay to free quarks and ant-quarks. A similar phenomenon for the baryon spectra is also seen by studying the energy of the D5 baryon wrapped on S^5 which is regarded as baryon.

In Sec. II, we give the setting of our model for our study, and a problem of the phase transition is discussed by solving the embedding of the D7 brane. In Sec. III, effective mass of the quark and the quark-antiquark potential are studied through the Wilson-Polyakov loop estimations. In Sec. IV, the possible bound state for the mesons and baryons are discussed. The summary is given in the final section.

*E-mail address: gouroku@dontaku.fit.ac.jp
†E-mail address: masafumi@higgs.phys.kyushu-u.ac.jp
‡E-mail address: nakamura@sci.kagoshima-u.ac.jp

II. BACKGROUND GEOMETRY AND D7 BRANE EMBEDDING

We solve the equations of motion for 10d IIB model retaining the dilaton Φ, axion χ and self-dual five-form field strength $F_{(5)}$. Under the Freund-Rubin ansatz for $F_{(5)}$, $F_{\mu_1\cdots\mu_5} = -\sqrt{\Lambda}/2\epsilon_{\mu_1\cdots\mu_5}$ [15,16], and for the 10d metric as $M_5 \times S^5$ or $ds^2 = g_{MN}dx^M dx^N + g_{ij}dx^i dx^j$, we can find the solution. The five dimensional M_5 part of the solution is obtained by solving the following 5d reduced action,

$$S = \frac{1}{2\kappa^2}\int d^5x\sqrt{-g}\left(R + 3\Lambda - \frac{1}{2}(\partial\Phi)^2 + \frac{1}{2}e^{2\Phi}(\partial\chi)^2\right), \tag{1}$$

which is written in the Einstein frame and taking $\alpha' = g_s = 1$. Then, we obtain, (see the Appendix A)

$$\begin{aligned} ds_{10}^2 &= G_{MN}dX^M dX^N \\ &= e^{\Phi/2}\left\{\frac{r^2}{R^2}A^2(-dt^2 + a(t)^2(dx^i)^2) + \frac{R^2}{r^2}dr^2 \right. \\ &\quad \left. + R^2 d\Omega_5^2\right\}, \end{aligned} \tag{2}$$

$$e^{\Phi} = 1 + \frac{q}{r^4}\frac{1 - (r_0/r)^2/3}{(1 - (r_0/r)^2)^3}, \qquad \chi = -e^{-\Phi} + \chi_0, \tag{3}$$

$$A = 1 - \left(\frac{r_0}{r}\right)^2, \qquad a(t) = e^{2(r_0/R^2)t}, \tag{4}$$

where $M, N = 0 \sim 9$ and $R = \sqrt{\Lambda}/2 = (4\pi N)^{1/4}$. As for the integration constants, r_0 denotes the horizon point, and it is related to the 4d cosmological constant λ as

$$\lambda = 4\frac{r_0^2}{R^4}. \tag{5}$$

And q is a constant which corresponds to the vacuum expectation value (VEV) of gauge fields condensate [9]. And other field configurations are set to be zero here. We notice that there is no singularity at the horizon r_0 in this case. This situation is similar to the black hole configuration used for the finite temperature gauge theory.

In the present configuration, the four dimensional boundary represents the inflational universe characterized by the 4d cosmological constant λ. So the above bulk-solution describes the gauge theory in the inflation universe. Firstly, we examine the properties of the flavor quarks in this gauge theory, and it is obtained by solving the embedding problem of the D7 brane in this background.

A. D7 brane embedding and phase transition

The D7 brane is embedded as follows. The extra six dimensional part of the above metric (2) is rewritten as,

$$\begin{aligned} \frac{R^2}{r^2}dr^2 + R^2 d\Omega_5^2 &= \frac{R^2}{r^2}(d\rho^2 + \rho^2 d\Omega_3^2 + (dX^8)^2 \\ &\quad + (dX^9)^2), \end{aligned} \tag{6}$$

where $r^2 = \rho^2 + (X^8)^2 + (X^9)^2$. We obtain the induced metric for D7 brane,

$$\begin{aligned} ds_8^2 &= e^{\Phi/2}\left\{\frac{r^2}{R^2}A^2(-dt^2 + a(t)^2(dx^i)^2) \right. \\ &\quad \left. + \frac{R^2}{r^2}((1 + (\partial_\rho w)^2)d\rho^2 + \rho^2 d\Omega_3^2)\right\}, \end{aligned} \tag{7}$$

where we set as $X^9 = 0$ and $X^8 = w(\rho)$ without loss of generality due to the rotational invariance in $X^8 - X^9$ plane. Then the embedding problem is reduced to obtain the solution for the profile function $w(\rho)$, and it is performed as follows.

The brane action for the D7-probe is given as

$$\begin{aligned} S_{\mathrm{D7}} &= -\tau_7\int d^8\xi\left(e^{-\Phi}\sqrt{-\det(\mathcal{G}_{ab} + 2\pi\alpha' F_{ab})} \right. \\ &\quad \left. - \frac{1}{8!}\epsilon^{i_1\cdots i_8}A_{i_1\cdots i_8}\right) \\ &\quad + \frac{(2\pi\alpha')^2}{2}\tau_7\int P[C^{(4)}]\wedge F\wedge F, \end{aligned} \tag{8}$$

where $F_{ab} = \partial_a A_b - \partial_b A_a$. $\mathcal{G}_{ab} = \partial_{\xi^a}X^M\partial_{\xi^b}X^N G_{MN}(a, b = 0 \sim 7)$ and $\tau_7 = [(2\pi)^7 g_s\alpha'^4]^{-1}$ represent the induced metric and the tension of D7 brane, respectively. And $P[C^{(4)}]$ denotes the pullback of a bulk four form potential,

$$C^{(4)} = \left(\frac{r^4}{R^4}dx^0\wedge dx^1\wedge dx^2\wedge dx^3\right). \tag{9}$$

The eight form potential $A_{i_1\cdots i_8}$, which is the Hodge dual to the axion, couples to the D7 brane minimally. In terms of the Hodge dual field strength, $F_{(9)} = dA_{(8)}$ [17], the potential $A_{(8)}$ is obtained.

When the gauge potentials A_a are neglected, the action is abbreviated as

$$S_{\mathrm{D7}} = -\tau_7\int d^8\xi\left(e^{-\Phi}\sqrt{\mathcal{G}} - \frac{1}{8!}\epsilon^{i_1\cdots i_8}A_{i_1\cdots i_8}\right), \tag{10}$$

and by taking the canonical gauge, we arrive at the following D7 brane action,

$$S_{\mathrm{D7}} = -\tau_7\int d^8\xi\sqrt{\epsilon_3}\rho^3 a(t)^3(A^4 e^{\Phi}\sqrt{1 + (w')^2} - C_8), \tag{11}$$

$$C_8(r) = \int^r dr' A^4(r')\partial_{r'}(\exp(\Phi(r'))) = \frac{q}{r^4}. \tag{12}$$

Then, finally, the equation of motion for $w(\rho)$ is obtained as,

$$\frac{w}{\rho + ww'}[\Phi' - \sqrt{1 + (w')^2}(\Phi + 4\log A)'] + \frac{1}{\sqrt{1 + (w')^2}} \times \left[w'\left(\frac{3}{\rho} + (\Phi + 4\log A)'\right) + \frac{w''}{1 + (w')^2}\right] = 0, \quad (13)$$

where prime denotes the derivative with respect to ρ. By solving this equation we find the profile of the embedded D7 brane and then we find simultaneously the quark properties, the quark mass m_q and the chiral condensate $\langle\bar{\Psi}\Psi\rangle$, where Ψ denotes the quark field. This point is shown below through various explicit solutions.

B. Trivial solution and chiral symmetry

Firstly we consider the asymptotic solution of w for large ρ. It is obtained usually as the following form

$$w(\rho) \sim m_q + \frac{c}{\rho^2}, \quad (14)$$

where m_q and c are interpreted from the gauge/gravity correspondence as the current quark mass and the chiral condensate, respectively, since the field ϕ^8 is corresponding to the conformal dimension three operators of the gauge theory. General solution of (13) is characterized by these two arbitrary parameters, m_q and c, since Eq. (13) is the second order differential equation of w although it is highly nonlinear. However, for a fixed m_q, we find one solution which is meaningful from the point of view of holography [9]. In other words, c is determined when m_q is fixed. This can be interpreted in the gauge theory as that $-c = \langle\bar{\Psi}\Psi\rangle$ is determined by a theory with a parameter m_q, the quark mass. Then the solutions for w are characterized only by the quark mass m_q, and the vev of quark condensate is determined uniquely by m_q.

However we must be careful in using the above asymptotic form (14) in solving the Eq. (13) since the form (14) is useful only for the case that CFT is realized on the boundary $r \sim \rho \to \infty$. In the present case, the geometry of the 4d boundary is dS_4 and the conformal symmetry is broken there, then the form (14) is not useful in getting the solutions of (13).

Actually, we find a solution of $m_q = 0$, and arbitrary c when we solve the Eq. (13) by expanding it in terms of the power series of $1/\rho^2$ with the asymptotic form of (14). Then, we find that the meaningful solution of $m_q = 0$ is nothing but the trivial solution, $w = 0$. The result is however nontrivial and important, because it implies that the chiral symmetry is preserved in the dS_4.

This point is understood from the fact that the attractive force is working between the D3 branes at the horizon and the D7 brane at $X^8 = w$. The force between them is obtained from the potential of w, which is obtained from the D7 action (11) by setting $w' = 0$ and remembering $r^2 = \rho^2 + w^2$ as follows,

$$V(w) = \tau_7(A^4 e^{\Phi} - C_8). \quad (15)$$

It represents the potential of w at fixed ρ, and typical examples for different qs are shown in the Fig. 1.

Then the force F between D3 and D7 branes is obtained

$$F = -\frac{\partial V}{\partial w} = -8\tau_7 \frac{w r_0^2}{r^4} A^3 e^{\Phi} < 0, \quad (16)$$

and we can see that the force is attractive at any point of ρ.

Then we can understand that the c must be negative for any solution of w. As a result, in the case of $m_q = 0$, we arrive at the trivial solution, $m_q = c = 0$ or $w = 0$ for nonzero λ. This situation is similar to the case of finite temperature gauge theory, but we find several different features through the nontrivial solutions between the finite temperature and finite cosmological constant case.

C. Nontrivial solutions and phase transition

However, the trivial solution is a part of solutions. In fact, we could find many nontrivial numerical solutions, whose behavior seems to be consistent with the asymptotic form of (14) at a glance. Some of them are shown in the Fig. 2–4 for different qs. In order to obtain these solutions in terms of the power series expansions, we must add correction terms of $\log(\rho)$ to the chiral condensate c and to the other coefficients of the power series of $1/\rho^2$. This improvement is naturally expected since the VEV, $c = -\langle\bar{\Psi}\Psi\rangle$, would receive this type of loop corrections due to the conformal noninvariance of the gauge theory in the present background dS_4.

Then, instead of (14), we find the following asymptotic form

$$w(\rho) \sim m_q + \frac{c_0 - 4m_q r_0^2 \log(\rho)}{\rho^2}, \quad (17)$$

where m_q and c_0 are arbitrary at this stage. However, c_0 would be determined by m_q and other parameters of the theory for the meaningful solution as stated above. The solutions of $w(\rho)$ and c for various m_q are shown by separating the solutions to three groups depending on the value of q.

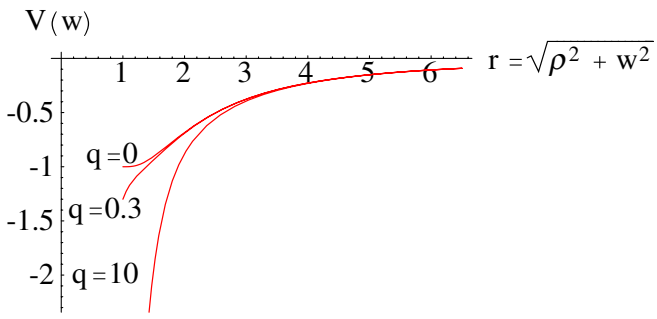

FIG. 1 (color online). Potential of w, $V(w) = A^4 e^{\Phi} + C_8$, for $q = 0$, 0.3 and 10 with $R = r_0 = 1.0$.

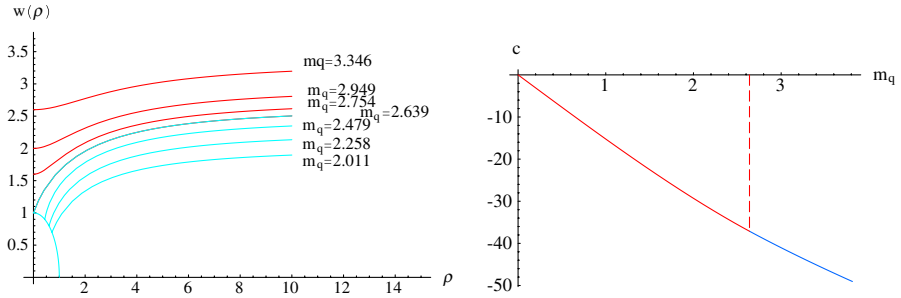

FIG. 2 (color online). Embedding solutions w and the chiral condensate c for $q = 0$ and $r_0 = R = 1.0$. For c, the cutoff is taken at $\rho = 100$, and the dashed line shows the transition point from group (a) to (b) at $m_q = 2.639$.

As for the c, in the present case, it depends on $\log(\rho)$ and diverges at $\rho = \infty$. So we need an appropriate subtraction or a renormalization for this quantity [14]. However, we estimate it as

$$c = c_0 - 4m_q r_0^2 \log(\rho_{\text{cutoff}}) \tag{18}$$

here by introducing an appropriate cutoff ρ_{cutoff} for the simplicity.

In any case, there is a horizon at $\rho^2 + w(\rho)^2 = r_0^2$ in the $\rho - w$ plane, and the embedded solutions are separated to two categories by the infrared end point of $w(\rho)$. In the first group, it is above the horizon (group (a)), and for the second, it is on the horizon (group (b)). This situation is also seen in the case of the finite temperature gauge theory.

The solutions are shown in the Fig. 2–4 for different qs and we find that all the solutions of w decreases with decreasing ρ, which means $c(= c_0 - 4m_q r_0^2 \log(\rho)) \leq 0$, for any solution. This is, as mentioned above, due to the attractive force between D3 and D7 branes, and $c = 0$ for $m_q = 0$ as expected. In the Fig. 1, we show the potential for the three different q cases for our understanding of this point. In other words, the chiral symmetry is preserved for $m_q = 0$ in any case. The numerical results are summarized as follows.

(i) $q = 0$: Firstly we consider the case of $q = 0$ or zero gauge-field condensate, shown in the Fig. 2, $\langle F_{\mu\nu}^2 \rangle = 0$. In this state, the quarks are not confined even in the limit of $\lambda = 0$. The second point to be noticed is that we could not find any jump of solutions when it changes from the group (a) to the group (b), and c changes smoothly at the transition point of m_q.
For finite q, the solutions for the group (b) are strongly restricted. Namely, the end point value of $w_0 \equiv w(\rho_0)$, where ρ_0 denote the value of ρ on the horizon, is constrained as (see Appendix B)

$$w_0 < \frac{r_0}{\sqrt{10}} \tag{19}$$

and the maximum of w_0 is realized in the limit $q \to 0$ but $q \neq 0$. We find solutions of $m_q < 0.96$ (in GeV) for $q = 10^{-7}$ and $r_0 = 1$. On the other hand, the solution for $q = 0$ and $r_0 = 1$ has $m_q > 2.4$, so there is a gap for the quark mass of groups (a) and (b). This gap decreases with increasing q, and we summarize the numerical results for $q > 0$ as follows.

(ii) Small $q(<2)$: We show in the Fig. 3 the solutions for nonzero but small q, namely, at $q = 0.3$. The ρ dependence of the solutions are similar to the $q = 0$ case, but there is a forbidden region of solutions for $2.118 < m_q < 2.683$ (in GeV) between the two solution groups of (a) and (b). This phenomena is characteristic to the present case of dS_4, and it has not been seen in the finite temperature case. This gap gradually decreases with increasing q and disappears for $q > 2$ as shown below.

(iii) Large $q(>2)$: In the Fig. 4, we show the solutions for large $q(= 10)$ case. In this case, the behavior of the

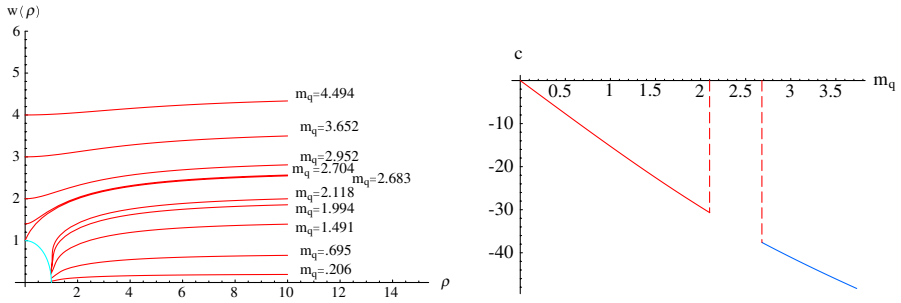

FIG. 3 (color online). For $q = 0.3$ and other parameter settings are the same with the above Fig. 2. The dashed lines in the right figure show the two critical points, $m_q = 2.683$ and $= m_q = 2.118$.

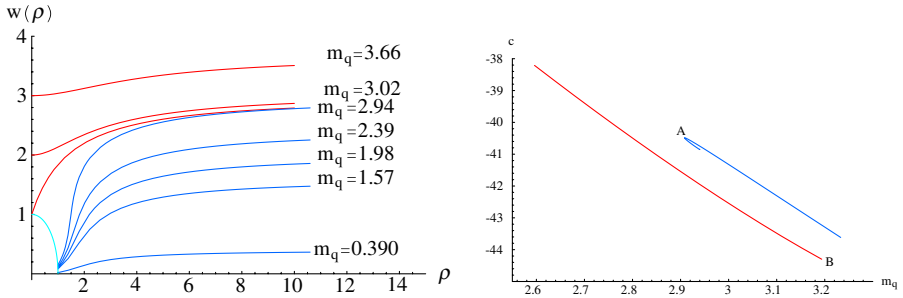

FIG. 4 (color online). For $q = 10$ and other parameter settings are the same with the above Fig. 2.

solutions is similar to the case of the finite temperature gauge theory. Namely, the forbidden band of the quark mass or a gap of $w(\infty)$ at the boundary seen in (ii) case disappears, but the gap at the infrared end point of w still remains and a phase transition as seen in the finite temperature case is expected when the solution translates from group (a) to the group (b). This is seen as a gap of the infrared end point w for the solution of common m_q at the transition point. In the present example, it is realized at $m_q = 2.94(\equiv m_c)$. This transition is also seen through the chiral condensate c, which is actually seen from the Fig. 4 as a jump of c at $m_q = m_c$. In the figure showing c, the upper one shows the one of solution group (a) and it begins with a gap at $m_q \sim 2.9$. And there is a narrow double valued region near the point A. In the multiple valued region of c, we choose the value of c, whose D7 energy is the minimum, as the plausible solution. The lower curve is obtained from the solutions of group (b) and it ends at $m_q \sim 3.2$, the point B. The similar gap is seen also in the mass spectra of mesons as seen below.

Next, we study the regularized D7 energy $E_{\rm D7}$ defined as

$$S_{\rm D7} = -\tau_7 \int d^7\xi \sqrt{\epsilon_3} a(t)^3 E_{\rm D7} \tag{20}$$

$$E_{\rm D7} = \int_{\rho_{\rm min}}^{\infty} d\rho \rho^3 (A^4 e^{\Phi} \sqrt{1 + (w')^2} - C_8), \tag{21}$$

in order to see the order of the phase transition which is clearly expected in the above calculation of case (iii) for $q(>2)$. The regularization for the D7 energy for the finite m_q solution is usually performed by subtracting the one of $m_q = 0$ [3], and the regularized energy $E^{\rm reg}_{\rm D7}(m_q)$ for the mass m_q is given as

$$E^{\rm reg}_{\rm D7}(m_q) = E_{\rm D7}(m_q) - E_{\rm D7}(0)$$
$$= \int_{\rho_{\rm min}}^{\rho_{\rm mutch}} d\rho \rho^3 \left(A^4 e^{\Phi} \sqrt{1 + (w')^2} - \frac{q}{r^4} \right)\Big|_{w(m_q)} \tag{22}$$

$$- \int_{r_0}^{\rho_{\rm mutch}} d\rho \rho^3 \left(A^4 e^{\Phi} - \frac{q}{\rho^4} \right)\Big|_{w=0} + \int_{\rho_{\rm mutch}}^{\infty} d\rho \Delta L_{\rm D7}, \tag{23}$$

where $\rho_{\rm mutch}$ represents the position where w is approximated well by its asymptotic form (17). In the present case, however, we need an extra subtraction term due to the cosmological constant r_0. In fact, in the large ρ region, the integrand $\Delta L_{\rm D7}$ is expanded by using asymptotic form of $w(\rho)$ as follows

$$\Delta L_{\rm D7} = 4 \frac{m_q^2 r_0^2}{\rho} + O(\rho^{-3}), \tag{24}$$

so we subtract here the first term in the estimation of $E^{\rm reg}_{\rm D7}(m_q)$. Then we obtain a small correction from the third term of Eq. (23).

The numerical results are shown in the Fig. 5–7. In the case of $q = 0$, we can see a small cusplike structure at the transition point between the two types of solutions (a) and

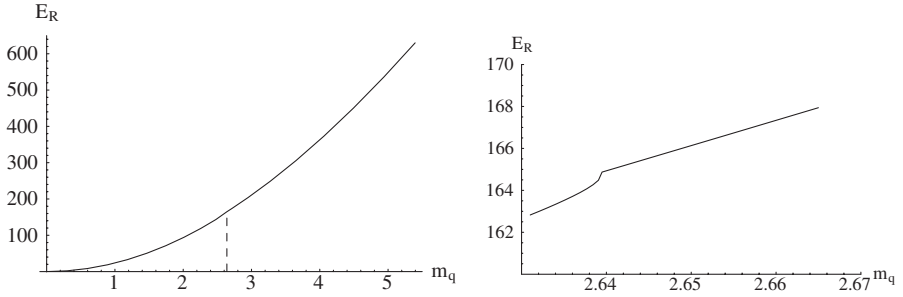

FIG. 5. The regularized energy for $q = 0$, and other parameter settings are the same with the above Fig. 2.

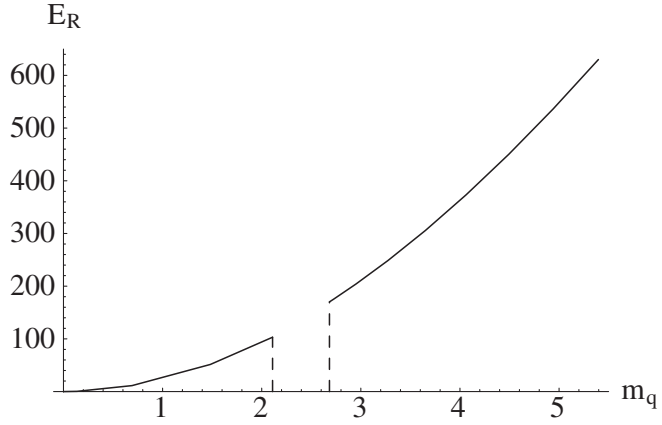

FIG. 6. The regularized energy for $q = 0.3$, and other parameter settings are the same with the above Fig. 2.

(b). This might imply some kind of phase transition. On the other hand, for $q = 10$, we find definite energy gap between the solutions of two groups at the same value of m_q in their overlap region. We then expect a first order phase transition from a solution of group (b) to the one of group (a) at an appropriate point of m_q. The details of these transitions observed here will be given in the future.

III. QUARK-ANTIQUARK POTENTIAL AND QUARK CONFINEMENT

We study a gravity description of quark-antiquark potentials in order to study the quark confinement. Before giving the calculation, we briefly review how quark-antiquark potentials described in the context of the gauge/gravity correspondence.

Consider the Wilson-Polyakov loop, $W = (1/N)\,\mathrm{Tr}Pe^{i\int A_0 dt}$, in $SU(N)$ gauge theory, then the quark-antiquark potential $V_{q\bar{q}}$ is derived from the expectation value of a parallel Wilson-Polyakov loop as $\langle W\rangle \sim e^{-V_{q\bar{q}}\int dt}$. Meanwhile, from the gravity side the expectation value is represented as

$$\langle W\rangle \sim e^{-S}, \tag{25}$$

in terms of the Nambu-Goto action

$$S = -\frac{1}{2\pi\alpha'}\int d\tau d\sigma\sqrt{-\det h_{ab}}, \tag{26}$$

with the induced metric $h_{ab} = G_{\mu\nu}\partial_a X^\mu \partial_b X^\nu$, where $X^\mu(\tau, \sigma)$ denotes the string coordinate.

Then the quark-antiquark potential can be calculated by setting the configurations of string coordinates under the background geometry given above. To fix the static string configurations of a pair of quark and antiquark, we choose $X^0 = t = \tau$ and decompose the other nine string coordinates into components parallel and perpendicular to the D3 branes:

$$\mathbf{X} = (\mathbf{X}_{||}, r, r\Omega_5). \tag{27}$$

Then the Nambu-Goto Lagrangian in the background (3) becomes

$$L_{\mathrm{NG}} = -\frac{1}{2\pi\alpha'}\int d\sigma e^{\Phi/2} \times\sqrt{A(r)^2 r'^2 + r^2 A(r)^2\Omega_5'^2 + \left(\frac{r}{R}\right)^4 A(r)^4 a(t)^2 \mathbf{X}_{||}'^2}, \tag{28}$$

where the prime denotes a derivative with respect to σ. The test string has two possible configurations: (i) a pair of parallel string, which connects horizon and the D7 brane, and (ii) a U-shaped string whose two end points are on the D7 brane.

A. Effective quark mass and confinement:

Firstly consider the configuration (i) of parallel two strings, which have no correlation each other. The total energy is then 2 times of one effective quark mass, $\tilde{m}_q$. As mentioned above, it is given by a string configuration which stretches between r_0 and the maximum r_{max}, so we can take as

$$r = \sigma, \qquad \mathbf{X}_{||} = \text{constant}, \qquad \Omega_5 = \text{constant}. \tag{29}$$

Then $\tilde{m}_q$ is obtained by substituting (29) into (28) as follows,

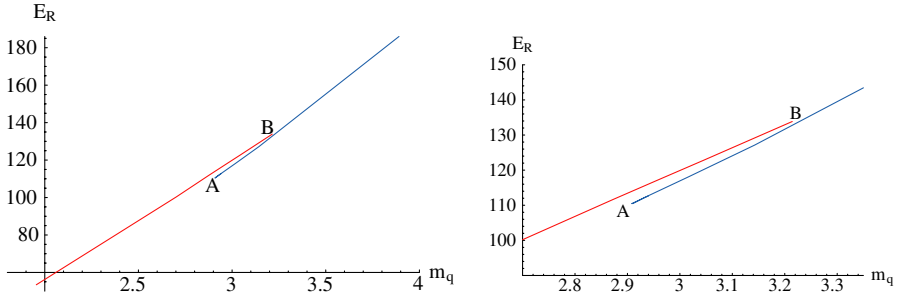

FIG. 7 (color online). The regularized energy for $q = 10$, and other parameter settings are the same with the above Fig. 2. The points A and B are the same points as the one in Fig. 4.

$$E = \frac{1}{\pi\alpha'}\int_{r_0}^{r_{\max}} dr e^{\Phi/2}A(r) = 2\tilde{m}_q, \tag{30}$$

where $r_{\mathrm{r\,max}}$ denotes the position of the D7 brane.

The integrand $e^{\Phi/2}A(r)$ is diverges at $r = r_0$ as $1/\sqrt{r-r_0}$, but we find that the contribution of this part to the integration vanishes,

$$\int_{r_0} dr \frac{1}{\sqrt{r-r_0}} = 2\sqrt{r-r_0}|_{r_0} = 0. \tag{31}$$

Then we find $\tilde{m}_q < \infty$ for finite r_0 or λ. This means that the quark is not confined in this case since single quark could exist. On the other hand, we find $\tilde{m}_q$ diverges for $r_0 = 0$ then the quark confinement.

While, in the above discussion, $q \neq 0$ is essential, we find for $q = 0$

$$2\tilde{m}_q = \frac{1}{\pi\alpha'}\frac{(r_{\max}-r_0)^2}{r_{\max}}. \tag{32}$$

Then the quark is not confined in this case even if $\lambda = 0$.

As for the cosmological constant dependence on $\tilde{m}_q$, the numerical calculations are shown in Fig. 8. From this figure, we find that (i) $\tilde{m}_q$ increases with q at any point of λ, and (ii) it decreases with increasing λ for any q.

B. *U*-shaped Wilson loop:

We now turn to the U-shaped configuration,

$$\mathbf{X}_{\parallel} = (\sigma, 0, 0), \qquad \Omega_5 = \text{constant}. \tag{33}$$

The equation of motion derived from the Lagrangian (28) with the configuration (33) are solved by

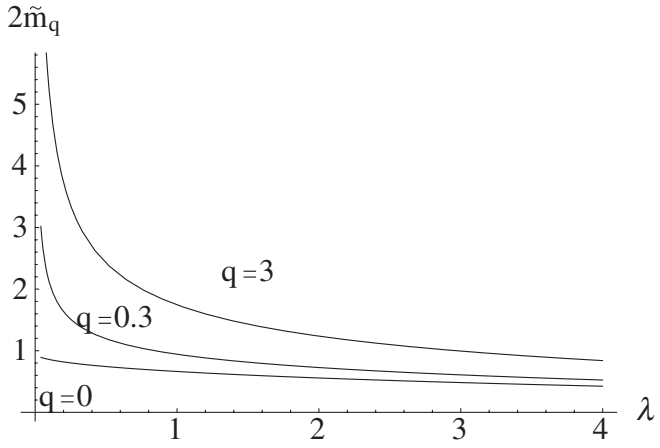

FIG. 8. $2\tilde{m}_q$ are shown for $R = 1$ (GeV^{-1}), $r_{\max} = 3$ and $\alpha' = 1$ (GeV^{-2}). The three curves are corresponding to the case of $q = 0$, 0.3 and 3, respectively.

$$e^{\Phi/2}\frac{1}{\sqrt{(r/R)^4A^2(r)a^2(t) + (dr/d\sigma)^2}}\left(\frac{r}{R}\right)^4 A^3(r)a^2(t) = \text{constant}. \tag{34}$$

The midpoint $r_{\min}$ of the string is determined by $dr/d\sigma|_{r=r_{\min}} = 0$. Then the distance and the total energy of the quark and antiquark are given by

$$L = 2R^2\int_{r_{\min}}^{r_{\max}} dr \times \frac{1}{r^2A(r)a(t)\sqrt{e^{\Phi(r)}r^4A(r)^4/(e^{\Phi(r_{\min})}r_{\min}^4A(r_{\min})^4) - 1}}, \tag{35}$$

$$E = \frac{1}{\pi\alpha'}\int_{r_{\min}}^{r_{\max}} \frac{A(r)e^{\Phi(r)/2}}{\sqrt{1 - e^{\Phi(r_{\min})}r_{\min}^4A(r_{\min})^4/(e^{\Phi(r)}r^4A(r)^4)}}. \tag{36}$$

Here we study the time independent distance $\tilde{L}$ defined as $\tilde{L} \equiv aL$ instead of L given above. The numerical results are shown in the Fig. 9

Two figures show the dependence of the energy E on the distance $\tilde{L}$ at the selected cosmological constant λ and q. For $\lambda = 0$, the well-known results are seen for $q = 0$ and finite q; (i) For $q = 0$, $E \propto 1/L$ at large L and $E \propto m_q^2 L$ at small L [3]. And for finite q [9], $E \propto \sqrt{q}L$ at large L and $E \propto m_q^2 L$ at small L. The behaviors at small L are common since the same AdS limit is realized there.

For finite λ, there is a maximum value of $L(= L_{\max})$ to find the U-shaped configuration. Namely, the U-shaped configuration disappears for $L > L(= L_{\max})$. The similar behavior is seen also in the case of the finite temperature [18]. In this sense, the theory in dS_4 is in the quark deconfinement phase as in the finite temperature case. However, we notice the following difference. In the case of finite temperature, there are two possible U-shaped string configurations at the same values of $L(<L_{\max})$, but in the case of finite cosmological constant, U-shaped string configuration is unique at a given value of $\tilde{L}(\tilde{L} < \tilde{L}_{\max})$. And at $\tilde{L} = \tilde{L}_{\max}$, the energy of this string configuration arrives at $2\tilde{m}_q$. Then, this implies that the U-shaped string configuration is broken for $L > L_{\max}$ to decay to free quark and antiquark. On the other hand, an unstable U-shaped string configuration is allowed for the finite temperature case even if $E > 2\tilde{m}_q$, and, just in this energy region, the other U-shaped string configuration is formed.

In our model, $\tilde{L}_{\max}$ is given as,

$$\tilde{L}_{\max} = \lim_{r_{\min}\to r_0} \tilde{L}, \tag{37}$$

and for $q = 0$, and we obtain

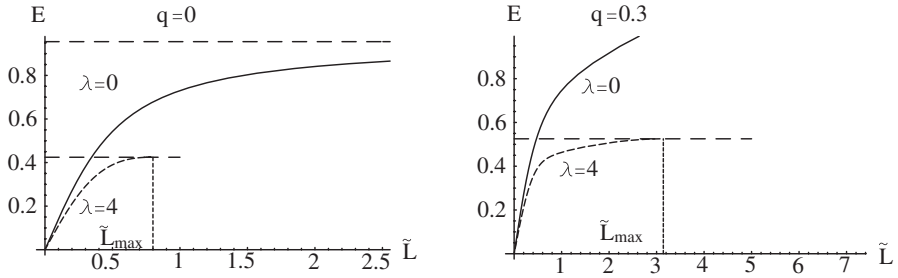

FIG. 9. Plots of E vs $\tilde{L}$ at $q = 0$ (the left figure) and $= 0.3$ (the right figure) (GeV^{-4}) for $R = 1$ (GeV^{-1}), $r_{\max} = 3$ (GeV^{-1}) and $\alpha' = 1$ (GeV^{-2}). The solid and dashed curves represent the case of $\lambda = 0$ and $\lambda = 4$ (GeV), respectively. The vertical solid and dashed lines represent the energy of two parallel straight strings.

$$\tilde{L}_{\max} = \frac{4}{\sqrt{\lambda}} \lim_{x_a \to 1} \int_{x_b}^{x_a} dx \frac{1}{(1-x^2)} \left(\frac{x_a^4 (1-x^2)^4}{x^4 (1-x_a^2)^4} - 1 \right)^{-(1/2)} \tag{38}$$

$$\sim \frac{\pi}{2} \frac{1}{\sqrt{\lambda}} \tag{39}$$

where

$$x \equiv \frac{r_0}{r}, \qquad x_a \equiv \frac{r_0}{r_{\min}}, \qquad x_b \equiv \frac{r_0}{r_{\max}}. \tag{40}$$

While the value of $\tilde{L}_{\max}$ in general depends on the lower bound x_b, however the approximate value seems to be independent of it. This is because of the fact that the integration is approximated by the value near the upper bound, x_a, of the integration. We can show the x_b independence of $\tilde{L}_{\max}$ directly by

$$\frac{\partial \tilde{L}_{\max}}{\partial x_b} = 0. \tag{41}$$

The numerical result is consistent with the one given in [14].

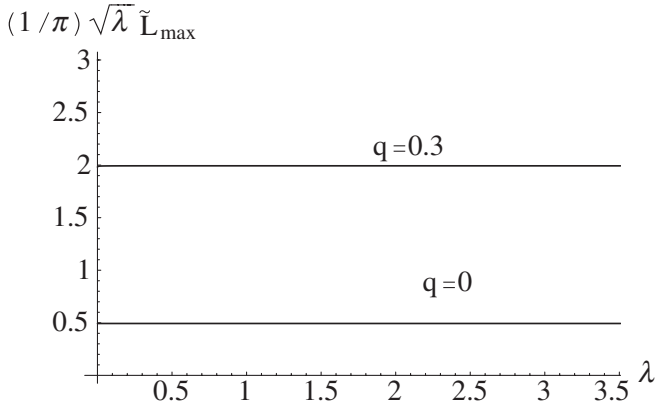

FIG. 10. Functional relation between $\frac{\sqrt{\lambda}\tilde{L}_{\max}}{\pi}$ and λ for $q = 0$ and $q \neq 0$.

As for $q \neq 0$, we get

$$\tilde{L}_{\max} = \frac{4}{\sqrt{\lambda}} \lim_{x_a \to 1} \int_{x_b}^{x_a} dx \frac{1}{(1-x^2)} \times \left(\frac{x_a^4 (1 + \tilde{q} x^4 \frac{(1-(1/3)x^2)}{(1-x^2)^3})(1-x^2)^4}{x^4 (1 + \tilde{q} x_a^4 \frac{(1-(1/3)x^2)}{(1-x_a^2)^3})(1-x_a^2)^4} - 1 \right)^{-(1/2)} \tag{42}$$

$$\sim \frac{2\pi}{\sqrt{\lambda}}, \tag{43}$$

where $\tilde{q} = q/r_0^4$. In this case also, we can show the $r_{\max}$ independence of $\tilde{L}_{\max}$ by (41), but the q independence of the above result is nontrivial. This point is understood from the fact that the dominant part of the integrand in this integration is independent of q. As a result, we get the result which is independent of $\tilde{q}$ and $r_{\max}$. But the approximate value is about 4 times of the one with $q = 0$. This is reduced to the difference of the quark-antiquark potentials at $\lambda = 0$ for $q = 0$ and $q \neq 0$. For the latter case $q \neq 0$, we obtain the linear potential at $\lambda = 0$. Their numerical values are also plotted in the Fig. 10 for $r_{\max} = 10$.

IV. POSSIBLE HADRON SPECTRUM

As shown in the previous section, while the theory is in the quark deconfined phase, the U-shaped string configuration exists. However, the energy of the configuration is bounded from the above by $2\tilde{m}_q$ which is the energy of the parallel string configuration. Its value depends on the cosmological constant, λ, and q. This situation implies the existence of stable meson states, the bound state of quark and antiquark, when their mass is below $2\tilde{m}_q$. We study this point by calculating the meson mass and comparing it with $2\tilde{m}_q$. We find a stable meson when its mass is smaller than $2\tilde{m}_q$ since this meson state can be expressed by the U-shaped string configuration, namely, as a bound state of quark and antiquark.

A. Meson spectra

The meson spectrum is obtained by solving the equations of motion of the fields on the D7 brane. According to [19], first we consider the fluctuations of the scalar mesons which are defined as,

$$X^9 = \tilde{\phi}^9, \qquad X^8 = w(\rho) + \tilde{\phi}^8.$$

And writing the wave functions in the following factorized form,

$$\tilde{\phi}^k = \phi^k(t, x^i)\phi^k(\rho)\mathcal{Y}_l(S^3) \qquad (k = 9, 8)$$

we get the linearized field equations for $\phi^9(\rho)$ and $\phi^8(\rho)$ as follows

$$\partial_\rho^2\phi^9 + \frac{1}{L_0}\partial_\rho(L_0)\partial_\rho\phi^9 + (1 + w'^2)\left[\left(\frac{R}{r}\right)^4\frac{m_9^2}{A^2} - \frac{l(l+2)}{\rho^2} - 2K_{(1)}\right]\phi^9 + (1 + w'^2)^{1/2}\frac{1}{r}\frac{\partial\Phi}{\partial r}\phi^9 = 0 \qquad (44)$$

$$L_0 = \rho^3 e^\Phi A^4\frac{1}{\sqrt{1 + w'^2}}, \qquad K_{(1)} = \frac{1}{e^\Phi A^4}\partial_{r^2}(e^\Phi A^4) \qquad (45)$$

and

$$\partial_\rho^2\phi^8 + \frac{1}{L_1}\partial_\rho(L_1)\partial_\rho\phi^8 + (1 + w'^2)\left[\left(\frac{R}{r}\right)^4\frac{m_8^2}{A^2} - \frac{l(l+2)}{\rho^2} - 2(1 + w'^2)(K_{(1)} + 2w^2K_{(2)})\right]\phi^8 + (1 + w'^2)^{3/2} \times\left[\left(2rK_{(1)}\frac{\partial\Phi}{\partial r} + \frac{\partial^2\Phi}{\partial r^2}\right)\frac{w^2}{r^2} + \frac{\partial\Phi}{\partial r}\frac{\rho^2}{r^3}\right]\phi^8 = -2\frac{1}{L_1}\partial_\rho(L_0ww'K_{(1)})\phi^8 \qquad (46)$$

$$L_1 = \frac{L_0}{1 + w'^2}, \qquad K_{(2)} = \frac{1}{e^\Phi A^4}\partial_{r^2}^2(e^\Phi A^4). \qquad (47)$$

Where four dimensional mass m_9 and m_8 are defined by

$$\ddot{\phi}^k(t, x^i) + 3\frac{\dot{a}}{a}\dot{\phi}^k(t, x^i) + \frac{-\partial_i^2}{a^2}\phi^k(t, x^i) = -m_k^2\phi^k(t, x^i). \qquad (k = 9, 8) \qquad (48)$$

In deriving the above equations of ϕ^8 and ϕ^9, we used

$$r^2 = \rho^2 + (\phi^8)^2 + (\phi^9)^2 + w^2 + 2w\phi^9. \qquad (49)$$

But we should notice here that the variable r in the above field equations is understood as $r^2 = \rho^2 + w^2$ since we are considering the linearized equations.

In Figs. 11(a), 11(c), and 11(e), the numerical results of the mass eigenvalues, m_9 (small point/thin line) and m_8 (large point/thick line), are plotted as functions of m_q. These values are all for the nodeless solutions, i.e. for the lowest mass state. The eigenvalues for $q = 0$, Fig. 11(a), show smooth variation with respect to m_q as expected from the solutions of its profile function (see the Fig. 2). For a nonzero but small value of q, $q = 0.3$, the mass eigenvalues are shown in the Fig. 11(c) for the region except for the forbidden range, $2.11 < m_q < 2.68$, which has been found and shown in Fig. 3 through the solutions of w. In Fig. 11(e), the results for $q = 10$ are shown. In this case, we could find the mass gap at the transition point of m_q (shown by dashed line), which is found through the solutions of w (see Fig. 4).

The next problem is to compare the mass eigenvalues m_9 and m_8 obtained with $2\tilde{m}_q$ as mentioned above in order to see the stability of the meson states. In Figs. 11(b), 11(d), and 11(f), m_9, m_8 and $E = 2\tilde{m}_q$ are plotted with respect to $r_0 = \sqrt{\lambda}/2$. In the case of $q = 0$ [Fig. 11(b)], m_9 and m_8 are larger than $2\tilde{m}_q$ at any point of λ. Then there is no stable meson state for $q = 0$. This is reasonable since the quark is not confined at $\lambda = 0$ for $q = 0$ and positive λ works to destroy the confinement phase. On the other hand, for $q > 0$, the quark is confined at $\lambda = 0$, then we expect stable mesons for small λ. In fact, in the case of $q > 0$, we could find the small λ region where the meson masses are smaller than $2\tilde{m}_q$. From Figs. 11(d) and 11(f), the stable regions are found as $r_0 = \sqrt{\lambda}/2 < 0.1(0.2)$ for $q = 0.3$ ($q = 10$). The critical value (or the upper bound) of λ increases with q as expected.

In our present universe, the value of $q^{1/4}$ is expected as the order of hadron mass since it provides the QCD string tension [9]. Meanwhile, λ is expected to be very small from the recent observation of small acceleration even if it exists. Then the mesons in the present world would not be affected by this small λ and all the mesons are stable. On the other hand, there would be no hadrons in the early universe which is inflationally expanding under a large λ. The quark and gluons would move almost freely in spite of their strong interactions which could combine them to make a bound state at $\lambda = 0$.

As for the vector field, its equation of motion is obtained from the action (8) as [19]

$$\partial_a(\sqrt{-\det g_{cd}}F^{ab}) - \frac{4\rho(\rho^2 + w^2)}{R^4}\varepsilon^{bjk}\partial_j A_k = 0, \qquad (50)$$

where ε^{ijk} is a tensor density (i.e., it takes values ± 1). The second term comes from the Wess-Zumino part of the action, proportional to the pullback of the RR five-form field strength, and is present only if b is one of the S^3 indices. And g_{ab} are metric in the Einstein frame.

Because of the existence of the cosmological constant, Lorentz invariance is broken. So, the resulting equations are different for a time component, space components and the components with S^3 indices even if $A_\rho = 0$ gauge is taken. But the final results are expected to be not so different from the scalar meson spectra. So, we abbreviate the analysis of vectors here.

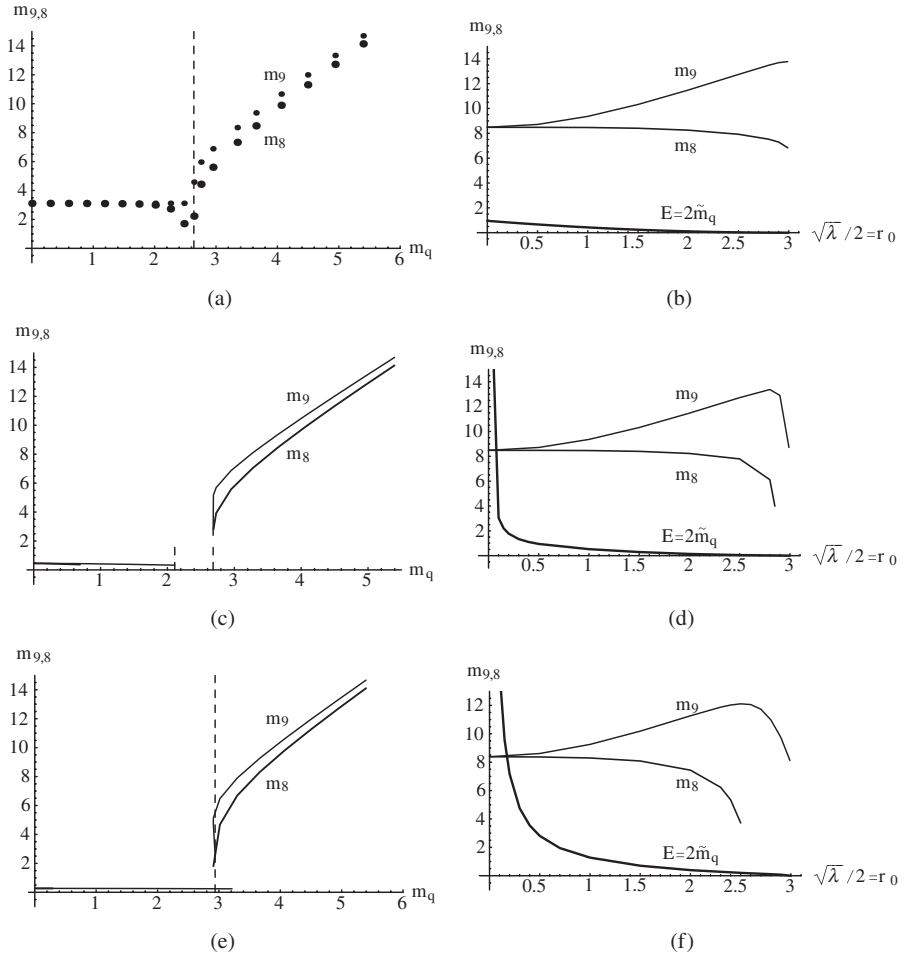

FIG. 11. $m_{9,8}$ vs m_q for $r_0 = 1.0$ and $R = 1$ and (a) $q = 0$, (c) $q = 0.3$, (e) $q = 10$. Small points denote m_9 while large points denote m_8 ((a)). Thin lines denote m_9 while thick lines denote m_8 ((c), (e)). Each vertical dashed line of the right of (a), (c) and (e) separates the region which touch the horizon and the region which do not touch the horizon. And $m_{9,8}$ vs $r_0 = \sqrt{\lambda}/2$ for $R = 1$ and $w(0) = 3.0$ and (b) $q = 0$, (d) $q = 0.3$, (f) $q = 10$. Thin line denotes m_9 while mid-thick lines denote m_8. Thick line denotes $E = 2\tilde{m}_q$.

B. Baryon

It has been shown that baryons correspond to D5-branes wrapped around the compact manifold M_5 [20,21]. Here we assume it to be S^5. The brane action of such a D5 probe is

$$S_{\mathrm{D5}} = -\tau_5 \int d^6\xi e^{-\Phi}\sqrt{\mathcal{G}}, \tag{51}$$

where $(\xi_i) = (X^0, X^5 \sim X^9)$, τ_5 represents the tension of D5 brane, and $\mathcal{G} = -\det(\mathcal{G}_{i,j})$ for the induced metric $\mathcal{G}_{ij} = \partial_{\xi^i} X^M \partial_{\xi^j} X^N G_{MN}$. The mass of the wrapped D5 brane is then

$$M_{\mathrm{D5}}(r) = \tau_5 e^{-\Phi}\sqrt{\mathcal{G}} = \tau_5 \pi^3 R^4 r A(r) e^{\Phi/2}. \tag{52}$$

Before seeing the λ dependence of this quantity, we consider the case of $\lambda = 0$,

$$M_{\mathrm{D5}}(r) = \tau_5 \pi^3 R^4 r\sqrt{1 + \frac{q}{r^4}}. \tag{53}$$

This has a global minimum $M_{\mathrm{D5}}(r_{\mathrm{min}}) = \tau_5 \pi^3 R^4 (4q)^{1/4}$,

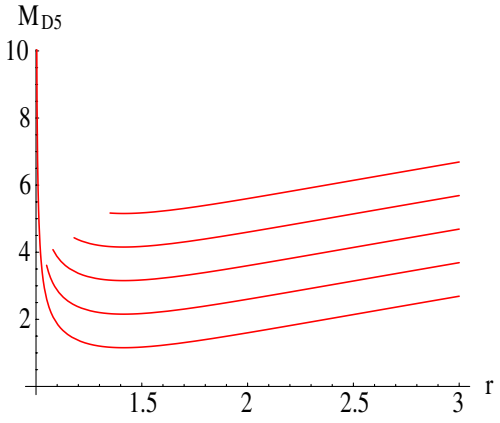

FIG. 12 (color online). The D5-brane mass $M_{\mathrm{D5}}(r)$ as a function of r. Here we set $q = 1$, $R = 1$ and $\tau_5 = 1/\pi^3 R^4$. The curves show the of $M_{\mathrm{D5}}|_{\lambda=4}$, $M_{\mathrm{D5}}|_{\lambda=4.41} + 1$, $M_{\mathrm{D5}}|_{\lambda=4.67} + 2$, $M_{\mathrm{D5}}|_{\lambda=5.57} + 3$ and $M_{\mathrm{D5}}|_{\lambda=7.29} + 4$ respectively, from bottom to top.

which is regarded as the baryon mass, at $r = r_{\rm min} = q^{1/4}$. Thus, the baryon mass is also induced by the q, i.e. by the gauge-field condensate. This is consistent with the fact that the QCD string tension is given by q in the present model.

Figure 12 shows the r dependence of $M_{\rm D5}(r)$ for five values of λ. For small side of λ, there exists a minimum at an appropriate point of r, and it disappears for large enough value of λ. Thus, there is a transition point of λ of confinement for the baryon as seen in the meson case.

V. SUMMARY

The Yang-Mills theory with light flavor quarks is investigated in the inflationally expanding 4d space-time or in the time-dependent dS_4 space-time. The flavor quarks are introduced by embedding the D7 brane as a probe in the background of the dual supergravity. The 10d background is deformed from $AdS_5 \times S^5$ by the dilaton and axion, and its 4d boundary of AdS_5 is set as the time-dependent dS_4 space-time with a 4d cosmological constant which is given as an arbitrary constant parameter in our model.

In this model, the conformal invariance is broken even at the ultraviolet boundary, then, in obtaining the D7 embedding, the asymptotic form of the profile function $w(\rho)$ must include logarithmic terms coming from the loop-corrections. Here we find the following form

$$w(\rho) \sim m_q + \frac{c_0 - 4m_q r_0^2 \log(\rho)}{\rho^2},$$

at the lowest order of large ρ limit, and this implies the VEV of the bilinear of quark fields, $\langle\bar{\Psi}\Psi\rangle$, receives the loop correction proportional to the cosmological constant λ and the quark mass m_q as

$$-\langle\bar{\Psi}\Psi\rangle = \frac{c}{R^4} = \frac{c_0}{R^4} - m_q \lambda \log(\rho). \tag{54}$$

This kind of correction would be expected in other quantities also, and we like to turn on this point in the future.

In terms of the above asymptotic form, we obtain various solutions of $w(\rho)$ with different values of m_q and c_0. And we find $c < 0$ for any solution of $m_q > 0$ and $c = 0$ for $m_q = 0$. This implies that the chiral symmetry is kept being unbroken for dS_4. The solutions are separated to two groups by their infrared end point whether it is above the horizon or just on the horizon. And when the solution is switched from the one group to the other, three kinds of behaviors are observed. For $q = 0$, the transition of the solutions is smooth, but there is a forbidden region of m_q for the case of small q. For large $q > 0$, on the other hand, we find a phase transition, at an appropriate value of m_q, and this is similar to the one observed in the finite temperature gauge theory.

In order to see the quark confinement, the Wilson-Polyakov loops are studied. Our model for $q > 0$ shows the quark confinement at $\lambda = 0$ since we find a linear rising potential with respect to the distance between quark and antiquark, L, in this case. On the other hand, in dS_4 or for $\lambda > 0$, the potential increases with L, but it disappears for large L, $L > L_{\rm max}$. We find that the energy of quark and antiquark system at $L = L_{\rm max}$ is equal to the one of two parallel strings, which connect horizon and the D7 brane. This means that the quark and antiquark do not make the bound state any more for $L > L_{\rm max}$ and they move freely and independently. In this sense, we can say that the gauge theory in dS_4 is in the quark deconfinement phase.

We should notice that, in the present finite λ case, the U-shaped string configuration is unique at a given value of L. This point is in sharp contrast to the case of finite temperature case, where there are two possible U-shaped string configurations at the same values of L. However, the energy of one of them is always higher than the one of the two parallel string configuration. In this sense, the stable U-shaped string configuration is unique in both cases, i.e. in the finite temperature and finite λ cases.

While the gauge theory of dS_4 is in the deconfinement phase, we expect that some meson states are stable for small λ due to the following reasons. The value of $L_{\rm max}$ proportional to $\lambda^{-1/2}$, so we will find a U-shaped string with long L at small λ. Secondly, the energy of the parallel string configuration $2\tilde{m}_q$ increases with decreasing λ. Actually, $\tilde{m}_q$ becomes infinite at $\lambda = 0$ for finite q. Then at small λ, $2\tilde{m}_q$ exceeds the meson mass considered. In order to assure this point, the spectra of mesons are examined through the fluctuations of D7 brane. Then, we can show that any meson state for a definite quark mass becomes stable when we take λ to be small enough.

As for the baryon, which is identified as D5 brane wrapped on S^5, its energy is obtained by the D5 brane action. We could find that their mass is induced by the gauge condensate q in our model. For finite λ, in the small side of λ, there exists a minimum of the D5 energy at an appropriate point of r, and it disappears at large value of λ. In this sense, we expect a transition point of λ of quark confinement for the baryon. The details of the transition point will be given in the future work.

ACKNOWLEDGMENTS

This work has been supported in part by the Grants-in-Aid for Scientific Research No. (13135223) of the Ministry of Education, Science, Sports, and Culture of Japan.

APPENDIX A

We start form the type IIB supergravity with the following bosonic action,

$$S = \frac{1}{2\kappa^2}\int d^{10}x\sqrt{-g}\Big(R - \frac{1}{2}(\partial\Phi)^2 + \frac{1}{2}e^{2\Phi}(\partial\chi)^2 - \frac{1}{4\cdot 5!}F_{(5)}^2\Big), \tag{A1}$$

where other fields are neglected since we need not them.

By taking the ansatz for $F_{(5)}$, $F_{\mu_1\cdots\mu_5} = -\sqrt{\Lambda}/2\epsilon_{\mu_1\cdots\mu_5}$ [15,16], and for the 10d metric as $M_5 \times S^5$ or $ds^2 = g_{MN}dx^M dx^N + g_{ij}dx^i dx^j$, the equations of motion are given as

$$R_{MN} = -\Lambda g_{MN} + \frac{1}{2}\partial_M\Phi\partial_N\Phi - \frac{1}{2}e^{2\Phi}\partial_M\chi\partial_N\chi, \quad \text{(A2)}$$

$$\frac{1}{\sqrt{-g}}\partial_M(\sqrt{-g}g^{MN}\partial_N\Phi) = -e^{2\Phi}\partial_M\chi\partial_N\chi g^{MN}, \quad \text{(A3)}$$

$$\frac{1}{\sqrt{-g}}\partial_M(\sqrt{-g}g^{MN}e^{2\Phi}\partial_N\chi) = 0, \quad \text{(A4)}$$

$$R_{ij} = \Lambda g_{ij}. \quad \text{(A5)}$$

Using the ansatz, $\chi = -e^{-\Phi} +$ constant, the Eq. (A2) is written as

$$R_{MN} = -\Lambda g_{MN}.$$

Then the metric of M_5 part is solved in the following form [22]

$$ds^2_{(5)} = \frac{r^2}{R^2}A^2(-dt^2 + a(t)^2(dx^i)^2) + \frac{R^2}{r^2}dr^2 \quad \text{(A6)}$$

$$A = 1 - \left(\frac{r_0}{r}\right)^2, \qquad a(t) = e^{2(r_0/R^2)t}. \quad \text{(A7)}$$

Using this result, Φ in the Eqs. (A4) and (A5) are solved as given in the Sec. II. We should notice that the integration constants are set appropriately in solving the equations.

Our model is based on type IIB supergravity, and we solved the equations of motion with dilaton and axion. In the present case, the model is reduced to 5d gauged supergravity. However, the solution given above breaks the supersymmetry since it is not a solution of the first order equations, which are written in terms of the superpotential $W(\Phi, \chi)$, which is a constant in the present case, of the 5d theory [23]. This is consistent with the fact that there is no supersymmetric theory in dS_4. We notice that the supersymmetry is also broken by our D7 brane embedding since the κ symmetry of the D7 brane action is lost [9].

APPENDIX B

Here we show the constraint given in Eq. (19) in the Sec. II. Suppose some solution $w(\rho)$ of the group (b), then its Infrared end point sits on the horizon at $\rho = \rho_0$. Then we expand $w(\rho)$ near the end point as

$$w(\rho_0 + \epsilon) = w(\rho_0) + w'(\rho_0)\epsilon + \cdots. \quad \text{(B1)}$$

By substituting this asymptotic form into the equation of w, Eq. (13), we obtain

$$w'(\rho_0) = \frac{\rho_0 + 3\sqrt{r_0^2 - 9w_0^2}}{r_0^2 - 10w_0^2}w_0, \quad \text{(B2)}$$

where $w_0 = w(\rho_0)$ and we used $\rho_0^2 = r_0^2 - w_0^2$. Since the physical solutions should be monotonically increasing with ρ in the present case, then we obtain $w_0 < r_0/\sqrt{10}$. This constraint does not depend on the value of q, while this does not appear for $q = 0$. In other words, this behavior is given by the nontrivial dilaton or the gauge condensate in the corresponding 4d gauge theory.

[1] J. M. Maldacena, Adv. Theor. Math. Phys. **2**, 231 (1998); S. S. Gubser, I. R. Klebanov, and A. M. Polyakov, Phys. Lett. B **428**, 105 (1998); E. Witten, Adv. Theor. Math. Phys. **2**, 253 (1998); A. M. Polyakov, Int. J. Mod. Phys. A **14**, 645 (1999).
[2] A. Karch and E. Katz, J. High Energy Phys. 06 (2003) 043.
[3] M. Kruczenski, D. Mateos, R. C. Myers, and D. J. Winters, J. High Energy Phys. 07 (2003) 049.
[4] M. Kruczenski, D. Mateos, R. C. Myers, and D. J. Winters, J. High Energy Phys. 05 (2004) 041.
[5] J. Babington, J. Erdmenger, N. Evans, Z. Guralnik, and I. Kirsch, Phys. Rev. D **69**, 066007 (2004).
[6] N. Evans, and J. P. Shock, Phys. Rev. D **70**, 046002 (2004).
[7] T. Sakai and J. Sonnenshein, J. High Energy Phys. 09 (2003) 047.
[8] C. Nunez, A. Paredes, and A. V. Ramallo, J. High Energy Phys. 12 (2003) 024.
[9] K. Ghoroku and M. Yahiro, Phys. Lett. B **604**, 235 (2004).
[10] R. Casero, C. Nunez, and A. Paredes, Phys. Rev. D **73**, 086005 (2006).
[11] S. Hawking, J. M. Maldacena, and A. Strominger, J. High Energy Phys. 05 (2001) 001.
[12] M. Alishahiha, A. Karch, E. Silverstein, and D. Tong, AIP Conf. Proc. **743**, 393 (2005).
[13] M. Alishahiha, A. Karch, and E. Silverstein, J. High Energy Phys. 06 (2005) 028.
[14] T. Hirayama, J. High Energy Phys. 06 (2006) 013.
[15] A. Kehagias and K. Sfetsos, Phys. Lett. B **456**, 22 (1999).
[16] H. Liu and A. A. Tseytlin, Nucl. Phys. **B553**, 231 (1999).
[17] G. W. Gibbons, M. B. Green, and M. J. Perry, Phys. Lett. B **370**, 37 (1996).
[18] K. Ghoroku, T. Sakaguchi, N. Uekusa, and M. Yahiro, Phys. Rev. D **71**, 106002 (2005).
[19] I. Brevik, K. Ghoroku, and A. Nakamura, Int. J. Mod. Phys. D **15**, 57 (2006).
[20] D. J. Gross and H. Ooguri, Phys. Rev. D **58**, 106002 (1998).
[21] E. Witten, J. High Energy Phys. 7 (1998) 006.
[22] I. Brevik, K. Ghoroku, S. Odintsov, and M. Yahiro, Phys. Rev. D **66**, 064016 (2002).
[23] D. Z. Freedman, S. S. Gubser, K. Pilch, and N. P. Warner, Adv. Theor. Math. Phys. **3**, 363 (1999).